13th World Conference on Earthquake Engineering
Vancouver, B.C., Canada
August 1-6, 2004
Paper No. 7007

SEISMIC LATERAL DEFORMATION AND ENERGY DEMANDS IN BARE AND INFILLED RC FRAMES

Laura LIBERATORE[1], Luis D. DECANINI[2] and Domenico LIBERATORE[3]

SUMMARY

In this paper, lateral deformation and energy demands of reinforced concrete frames when subjected to several earthquake ground motions are evaluated by means of numerical analyses. More precisely, 4-storey, 2-bay RC frames, designed for (i) static vertical loads only, and (ii) seismic actions, are studied considering three different conditions, namely bare frame, fully infilled frame and open ground story configuration. Six real accelerograms are considered, focusing on near-fault records. The main outcomes are presented and compared with the demand imposed on single-degree-of-freedom systems. Moreover, the demands imposed on the analyzed models are compared with the corresponding capacities, in order to evaluate the reached structural damage level. It is concluded that the structures benefit a lot from the presence of regularly distributed infills. The presence of an open story is strongly detrimental for the frame designed for vertical loads only, while the aseismic structure is less affected by this irregularity in the infills distribution. The comparison between the displacement and energy demand for MDOF systems with the demand for SDOF systems showed interesting trends, but also large dispersions.

INTRODUCTION

In recent years the interest in displacement design procedures has been growing. In fact, it is well known that lateral displacements due to earthquake ground motion can produce structural and non structural damage. Besides the lateral deformation demand, the energy demand imposed by seismic excitation plays an important role during severe earthquakes; in particular, the hysteretic energy is a measure of inelastic energy dissipation and includes cumulative effects of repeated cycles of inelastic response and can be associated to the expected structural and non structural damage.
With the aim of analyzing the dynamic behavior of RC buildings, numerical analyses are performed and both the lateral displacement and the energy demand imposed on buildings during earthquake ground motions are estimated. The attention is focused on two main aspects, the former being the evaluation of the behavior of structures designed with no seismic actions, compared with aseismic structures, the latter being the assessment of the influence of infill masonry panels. In infilled frames, the infills can control the global seismic response, providing most of the earthquake resistance and preventing collapse of weak structures, as observed after many earthquakes. Therefore, it seems of prominent importance to evaluate

[1] Ph.D, Dept. of Structural and Geothecnical Engineering - University of Rome “La Sapienza”.
[2] Full Professor, Dept. of Structural and Geothecnical Engineering - University of Rome “La Sapienza”.
[3] Full Professor, DiSGG, University of Basilicata.

the effects due to the infills and their possible irregularities, which may be present from the design or may rise during earthquakes, due to loss of infills panels caused by out-of-plane collapse, or, for high level of the excitation, by the in-plane failure.
The results have been checked mainly with damages observed after earthquakes, since the available experimental data based on shaking table tests or pseudo-dynamic tests are scarce for the infilled frames.

TEST STRUCTURES

Description of the Analyzed Structures

The study presented in this paper deals with two-span, four stories reinforced concrete frames. Two types of frame are examined: the former, indicated as "non-seismic", designed for static vertical loads only, so as to represent many Italian existing building, the latter, indicated as "seismic", designed for seismic actions, as described in the following. For each frame, three conditions are considered, namely bare frame, fully infilled frame and open ground story configuration, as indicated in Figure 1. The presence of the infills and their possible irregularities are neglected in the design, i.e. size and reinforcement of beams and columns are the same for bare and infilled frames.
The vertical static loads used for design are those of an inner frame of a building with 5 m spacing between frames. For the design of the seismic frame, seismic equivalent static loads have been applied, considering a seismic coefficient of 0.22, corresponding to an effective acceleration of about 0.35g and a behavior factor of 4. Design criteria, such as capacity design and local ductility criteria, prescribed by many current codes, have not been explicitly applied, even though minimum conditions for the longitudinal bars and the stirrups, prescribed by the past Italian code, have been satisfied. A cylindrical compressive strength of 21 MPa for the concrete and a yield strength of 375 MPa for the steel are considered. Member cross-sectional size for the different structures analyzed are shown in Table 1.

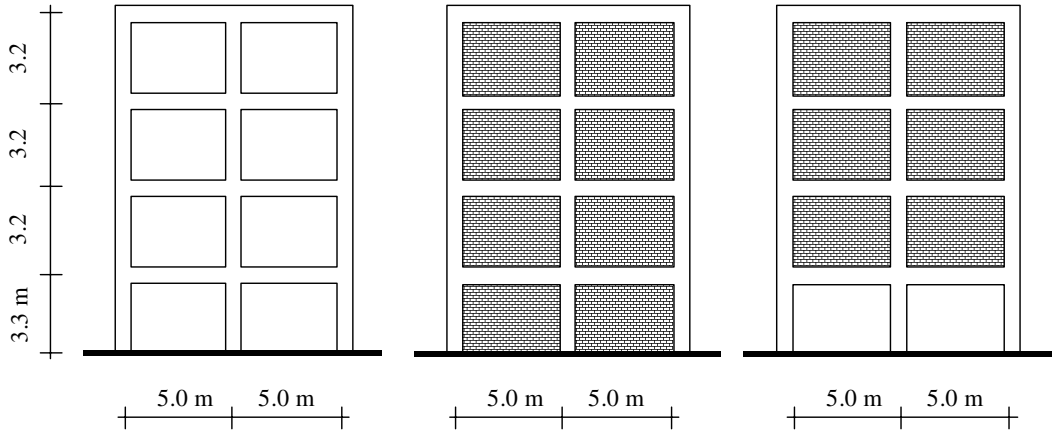

Figure 1: Test structures: bare, fully infilled and open-story frames.

Table 1: Columns and beams cross-sectional size (cm).

Frame	Level	Inner columns	Outer columns	Beams b/h
Non-seismic	1st and 2nd	30 x 30	30 x 30	50/20
	3rd and 4th	25 x 25	25 x 25	50/20
Seismic	1st and 2nd	35 x 35	35 x 35	20/50 + slab
	3rd and 4th	35 x 35	30 x 30	20/50 + slab

To investigate the influence of the infills, a masonry, deemed representative in terms of strength and stiffness of those used in several South-European countries, is considered. Specifically a masonry made of

hollow bricks with thickness 145 mm and by a mortar of cement and sand (Pires [1]), is adopted. The mechanical properties of masonry are: compressive strength, f_{mk} = 2.10 MPa; shear strength, evaluated through diagonal compressive test, f_{vk} = 0.40 MPa; initial elastic modulus, E_m = 1880 MPa.

Numerical models

Nonlinear dynamic, nonlinear pushover and linear modal analyses were performed by using a finite element code with fiber elements, which allow the detailed modeling of steel and concrete constitutive laws, account for N-M interaction and are used for both the RC elements and the infills, as described below.

Model of RC elements

Reinforced concrete elements are subdivided and modeled through fiber elements: columns and beams are divided in a number of sub-elements and each cross-section element is further subdivided into an appropriate number of concrete and steel fiber, at each fiber is then assigned an appropriate constitutive law. At element ends, i.e. at beam-column joints, rigid links are used.

The concrete constitutive laws are defined by making use of the modified Kent & Park model [2], which provides the maximum compressive strength, the strain at maximum compressive strength, the confined concrete ultimate strain values, ε_{cu}, associated to a residual stress equal to 20% of the peak value as function of the: cylindrical compressive strength, cross-sectional dimensions, spacing and dimension of the stirrups, steel yield strength. Different laws are adopted according to the dimensions and transversal reinforcement of the element section. The values of ε_{cu} ranges between 8.4% and 29.2%, determining different slopes for the softening branch. The hysteretic behavior takes into account stiffness degradation.

A tri-linear curve is used to define the steel force-deformation envelope, considering an elastic modulus equal to 190 kN/mm^2. The Bauschinger effect is indirectly taken into account by assigning the value of 95 kN/ mm^2 to the second branch of the envelope, up to a strain equal to 3%. Finally, an hardening ratio of 2% is considered.

Model of masonry panels

The infill panels are included as equivalent diagonal no tension struts. The struts are modeled through fiber elements, with a section composed by a single fiber, assuming specific constitutive and hysteretic laws.

The Decanini et al. [3] strut model, which takes into account the cyclic nature of seismic action, is adopted. It provides: strength, secant stiffness and thickness of the equivalent strut as function of different geometrical and mechanical parameters of the bare-infill system, thus accounting for the interaction between structural elements and infills masonry. The values obtained for the analyzed structures, being dependent on the dimension and mechanical characteristics of the frame, are different for the seismic and the non-seismic frame and for different levels: the equivalent strut lateral strength ranges between 157 kN and 162 kN while the secant stiffness ranges between 35 kN/mm and 49 kN/mm.

The original model is updated to include the post-cracking behavior (softening branch) and the degrading cyclic behavior. The adopted model takes into account the main features of the cyclic behavior of masonry, such as the degradation of strength under displacement cycles of constant amplitude and the degradation of stiffness in the unloading branches, as function of the maximum deformation and of the dissipated energy, according to a relationship similar to that proposed by Park et al. [4].

The constitutive and hysteretic laws are checked through comparisons between numerical and laboratory test results.

SEISMIC INPUT

The study is focused mainly on the analysis of ground motion effects in near-fault condition. Six natural input motions are used, as indicate in Table 2, where M_S and M_W are the surface wave magnitude and the moment magnitude, respectively, D_f is the closest distance from the surface projection of rupture and I_{MCS} is the MCS macroseismic intensity ($I_{MCS} \cong I_{MM} + 1$). Three records come from the recording station of Calitri (Campania-Basilicata, Italy, 1980), the others are relevant to the Imperial Valley 1976, Kocaeli 1999 and Northridge 1994 earthquakes. The CALITWE record, which has a total duration of 70 s, consists of two different shocks: the former, CAL0-35, with a duration of 35 s, was caused by a fault at 20.5 km from the site; the latter, CAL40S, caused by the rupture of a fault at 6 km from the site. In the analyses, the sub-events are considered both separately and subsequently (CALITWE).

Table 2: Records used for the numerical analyses.

Earthquake	M_s	M_w	Slip type	Station	D_f (km)	Soil type	I_{MCS}
Campania-Basilicata (Italy, 11/23/1980)	6.6	6.6	Normal	CAL0-35	20.5	Intermediate	VIII-IX
Campania-Basilicata (Italy, 11/23/1980)	6.0	6.0	Normal	CAL40S	6.0	Intermediate	VIII-IX
Campania-Basilicata (Italy, 11/23/1980)	6.8	6.8	Normal	CALITWE	20.5–6.0	Intermediate	IX
Imperial Valley (USA, 10/15/1979)	6.9	6.5	Strike-slip	CRU230 (El Centro #8)	3.5	Intermediate	IX-X
Kocaeli (Turkey, 08/17/1999)	7.8	7.4	Strike-slip	YPT330 (Yarimca)	2.6	Soft	X
Northridge (USA, 01/17/1994)	6.8	6.7	Reverse	RRS318 (Rinaldi)	2.3	Intermediate	XI

Some parameters characterizing the selected accelerograms are listed in Table 3, where: EPA is the effective acceleration, given by the average pseudo-acceleration in the range of period 0.1-0.5 s, divided by 2.5; I_H is the Housner Spectral Intensity, given by the integral of the 5% damped spectral pseudo-velocity in the range of periods 0.1÷2.5 s; t_d is the effective duration according to Trifunac & Brady; AEI(0-2) (Decanini & Mollaioli [5]) is given by the integral of the absolute elastic input energy per unit mass (5% damped) in the range of periods 0-2 s; EI_{max} is the maximum elastic input energy and $EH_{max\text{-}\mu=2}$ is the maximum hysteretic energy demand for an EPP oscillator with ductility equal to 2; T_{EImax} and T_{EHmax} are the periods where the above mentioned maximum values occur.

Table 3: Records used for the numerical analyses.

Record	PGA (g)	EPA (g)	PGV (cm/s)	I_H (cm)	t_D (s)	AEI(0-2) (cm^2/s)	EI_{max} (cm^2/s^2)	T_{EImax} (s)	$EH_{max\text{-}\mu=2}$ (cm^2/s^2)	T_{EHmax} (s)
CAL0-35	0.14	0.15	21	101	24.84	8900	9300	0.95	3300	0.95
CAL40S	0.18	0.14	32	116	17.68	6500	6300	1.65	2000	1.25
									2000	1.55
CALITWE	0.18	0.16	32	118	45.93	15000	13700	0.95	3724	0.90
							12700	1.60	4014	1.60
CRU230	0.45	0.33	50	125	5.81	6900	6600	0.60	2200	0.60
							13700	4.50	4200	4.00
YPT330	0.35	0.21	62	177	15.61	17900	24500	1.45	8500	1.40
							40000	3.50	12600	3.40
RRS318	0.47	0.47	84	296	7.86	29600	32000	1.30	13500	1.20
							30000	2.25	11200	2.20

In Figure 2 there are shown the elastic input energy spectra and the hysteretic energy spectra (5% damped). The input energy and the hysteretic energy demand are higher for the RRS318 and YPT330 records, even though the maximum value corresponding to YPT330 occurs at a period greater of that of the examined structures. Figure 3 shows the pseudo-acceleration spectra and the elastic displacement spectra for the six accelerograms. It seems worthwhile to highlight that the maximum values of pseudo-acceleration occur at periods which are significantly different from the corresponding input energy peaks.

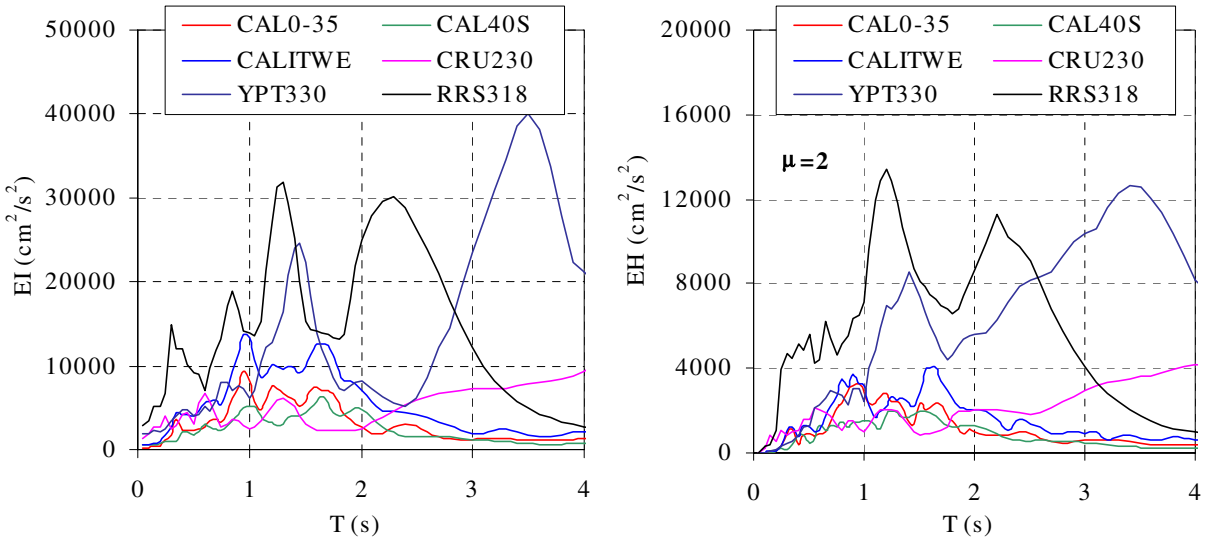

Figure 2: Elastic input energy spectra, EI and hysteretic energy spectra, EH.

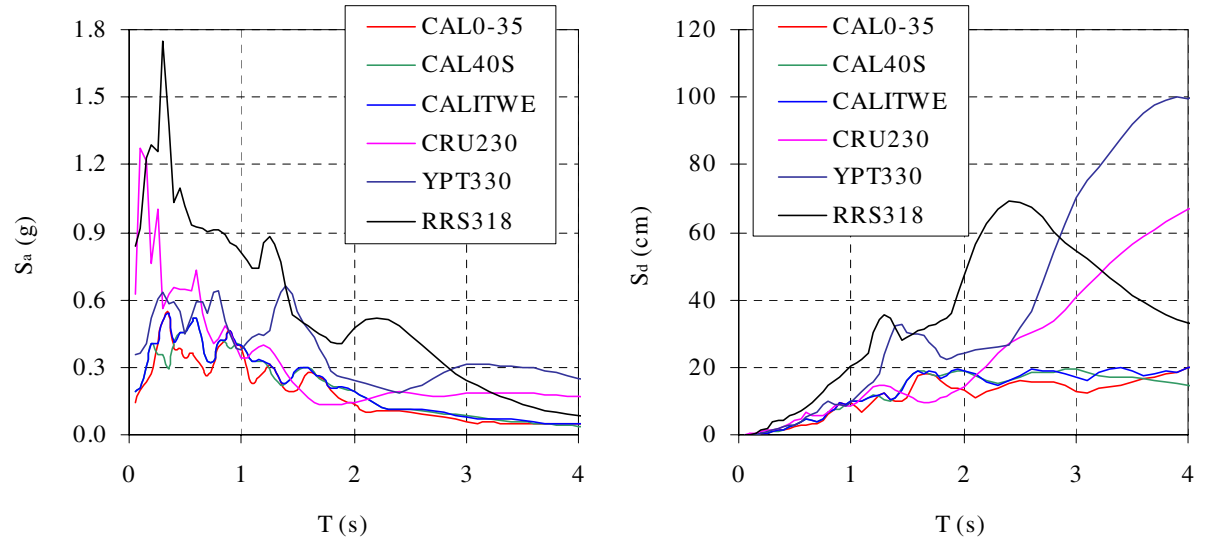

Figure 3: Pseudo-acceleration spectra, S_a, and elastic displacement spectra, S_d.

RESULTS

As mentioned before, the structural response is studied mainly through the analysis of displacements and energies parameters, such as the interstory drift, the top displacement and the energy dissipated through inelastic deformations, as these factors are deemed to be correlated to the structural and non-structural damage. The results of the nonlinear dynamic analyses are illustrated and compared with the demands imposed on SDOF systems. Finally, the demands imposed on the analyzed models are compared with the corresponding capacities, in order to evaluate the damage level.

Lateral Displacements Demand

The maximum interstory drift values, δ_{max}, are reported in Table 4 while Figures 4 and 5 show the maximum interstory drift profile along the height of the buildings. For the YPT330 record, the analysis of the non-seismic frames with open story stopped before the end of the accelerogram due to convergence problem; therefore the drift values reported are smaller of the attained ones. For the other accelerograms, the values represent the maximum obtained during the whole dynamic analysis and can be considered as the drift demand imposed by the seismic excitations. These values are compared with the "drift limits", considered related to a high level of damage and set equal to 2.5% for the bare frames, 1.8% for the open story frames and 1.5% for the fully infilled ones. Cases in which the maximum drift is greater than the drift limit are highlighted in bold letters in Table 4.

Table 4: Maximum interstory drifts for non-seismic ($\delta_{maxNonSeis}$) and seismic ($\delta_{maxSeis}$) frames.

Record	Bare frames			Fully infilled			Open story		
	$\delta_{maxNonSeis}$ (%)	$\delta_{maxSeis}$ (%)	$\delta_{max\ Seis.}/\delta_{maxNonSeis}$	$\delta_{maxNonSeis}$ (%)	$\delta_{maxSeis}$ (%)	$\delta_{max\ Seis.}/\delta_{maxNonSeis}$	$\delta_{maxNonSeis}$ (%)	$\delta_{maxSeis}$ (%)	$\delta_{max\ Seis.}/\delta_{maxNonSeis}$
CAL0-35	2.31	1.25	0.54	0.59	0.16	0.27	**2.25**	0.69	0.31
CAL40S	2.03	1.50	0.74	0.58	0.06	0.10	**3.26**	1.05	0.32
CALITWE	**2.59**	1.53	0.59	0.91	0.16	0.18	**3.01**	1.05	0.35
CRU230	**3.70**	1.81	0.49	0.66	0.31	0.47	**3.18**	1.30	0.41
YPT330	**5.09**	**3.09**	0.61	0.94	0.28	0.30	**>3.61**	1.71	<0.47
RRS318	**6.94**	**3.75**	0.54	**4.48**	1.09	0.24	**7.29**	**4.43**	0.61

It can be seen that the deformations of the structures are noticeably influenced by the design, the presence of infills and the presence of an open story. The main outcomes are summarized in the following:

1. Considering the mean values (mean of the six records), the maximum interstory drift for the bare seismic frames is equal to about 60% of that found for the bare non-seismic frames; this difference increases when masonry infills are present: for the seismic frame the drifts are equal to 25% (open story frame) and 40% (fully infilled frames) of the non-seismic counterpart.
2. The masonry, if uniformly distributed along the height, strongly decreases the lateral displacements demand with mean reductions equal to 70% and 85% for the non-seismic and seismic frames, respectively. Anyway, it must be pointed out that the maximum shear obtained in the columns of the fully infilled non-seismic frames is very close to their shear strength, due to the high shear force transmitted by the masonry panels.
3. For the seismic infilled frame, the maximum drift is always smaller of the drift limit, while for the bare seismic frame the limit is exceeded for the YPT330 and RRS318 records, and in the case of open story configuration is exceeded for the RRS318.
4. For the non-seismic frames, the drifts are always greater of the drift limit when the open story is present, while for the fully infilled frame this situation occurs only for the RRS318 accelerogram. For the bare non-seismic frame, the limit is always exceeded, except for CAL0-35 and CAL40S.

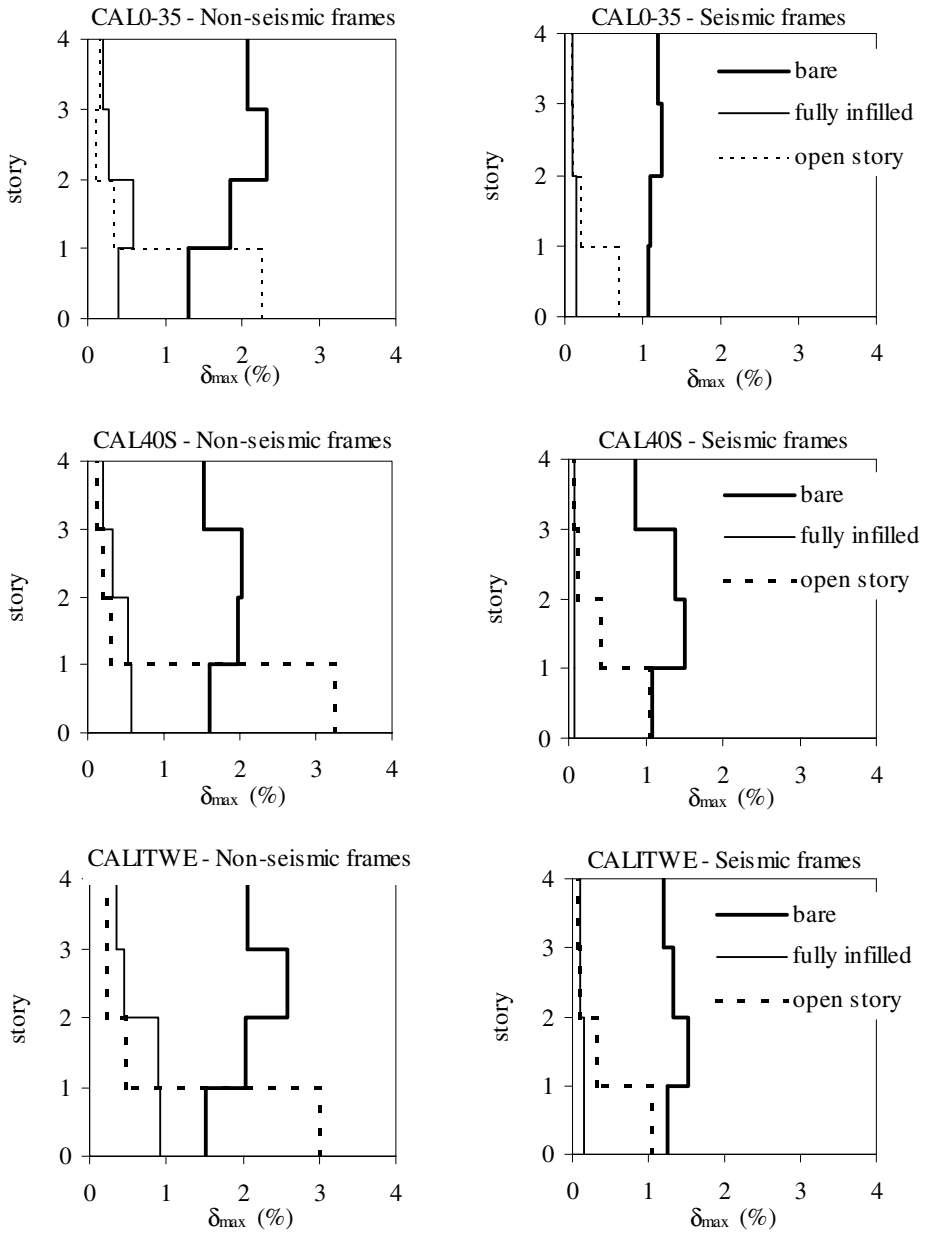

Figure 4: Maximum interstory drift, δ_{max} (%) – Calitri records.

Figures 4 and 5 show that, in general, the maximum values of drift are attained at the second or third story for the bare frames, at the first or second story for the infilled ones and, as expected, at the first story for the open story frames. It is interesting that for the seismic frame the maximum drifts in the bare frames are similar or slightly greater of that obtained for the open story counterpart, with the exception of the RRS318 record, while for the non-seismic frames the presence of the open story is strongly detrimental. The negative influence of the open story increases when the ratio between the masonry lateral strength and the frame strength increases, being equal to 0.98 for the seismic frame and to 2.33 for the non-seismic frame.

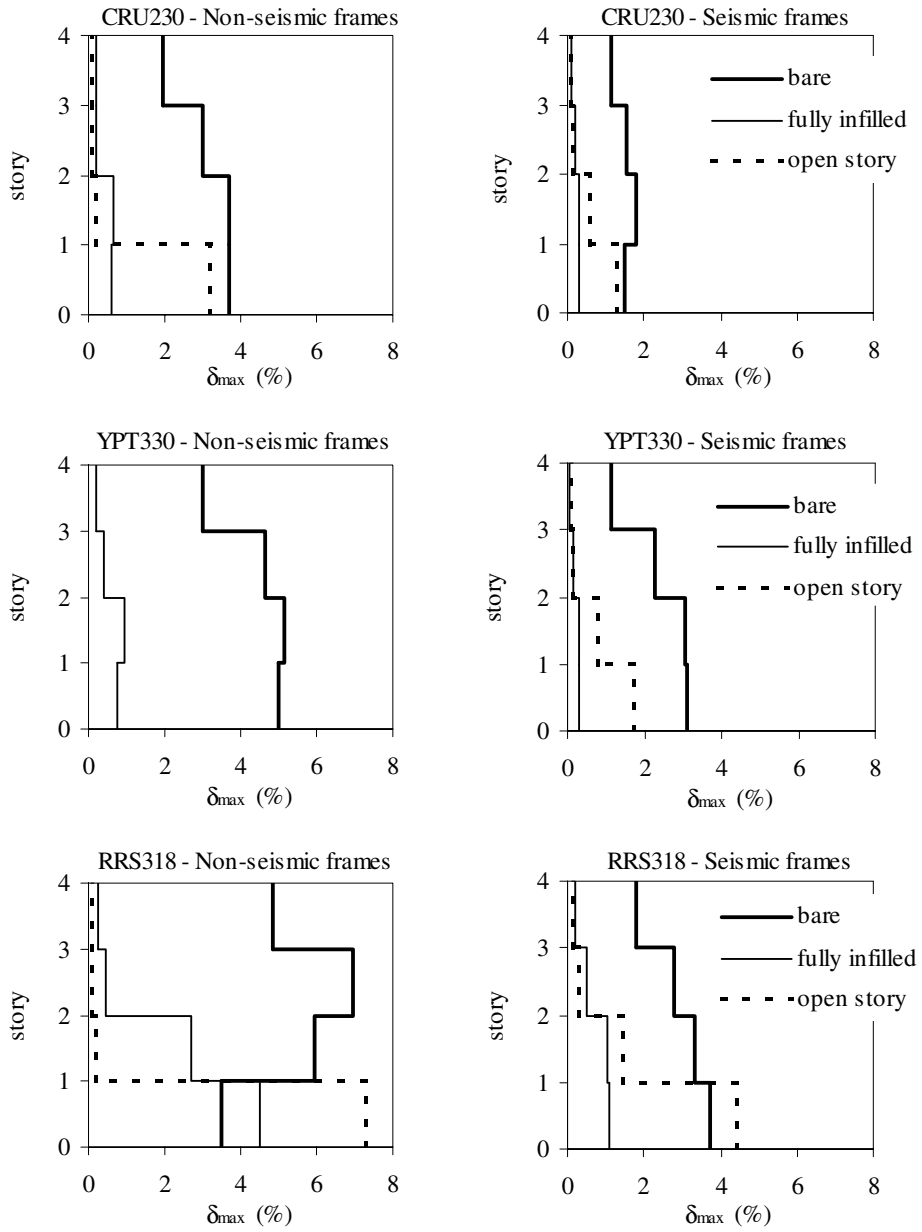

Figure 5: Maximum interstory drift, δ_{max} (%) – CRU230, YPT330, RRS318.

In Table 5 there are shown the maximum values of top displacement divided by the total height, $\delta_{top}= \Delta_{top}/H$, and the Coefficient of Distortion, COD, while the mean and standard deviation of COD for the six considered accelerograms are reported in Table 6. The COD, defined as the ratio between δ_{top}, and the maximum interstory drift, δ_{max}, is an indicator of the difference between the actual displacement distribution over the height of the structure and the linear distribution, and can provide direct information about localized deformation. The reported values show that for the bare frames, both seismic and non-seismic, the COD mean value is equal to 1.35, while the standard deviation is equal to 0.09; the mean value is consistent with that obtained in the test performed by Negro & Verzelletti [6] and in numerical analysis carried out by Panagiotakos & Fardis [7]. When uniformly distributed infills are present, the COD increase, compared to the bare frames, especially for the non-seismic frame, where the COD mean value is 1.74. As expected, the highest values of COD are found for the open story configuration, the mean value

being equal to 2.74 for the seismic frame and 3.50 for the non-seismic frame. Finally, the COD is found to be not dependent on the seismic excitation damage potential, as also found by Panagiotakos & Fardis for bare frames [7].

Table 5: Maximum top displacement, δ_{top}, and coefficient of distortion, COD.

Non-seismic frames

Record	Bare frames		Fully infilled		Open story	
	δ_{top} (%)	COD	δ_{top} (%)	COD	δ_{top} (%)	COD
CAL0-35	1.71	1.35	0.35	1.69	0.68	3.31
CAL40S	1.48	1.37	0.36	1.61	0.90	3.62
CALITWE	1.71	1.51	0.64	1.42	0.99	3.04
CRU230	2.84	1.30	0.40	1.65	0.88	3.61
YPT330	4.21	1.21	0.53	1.77	>0.99	(3.65)
RRS318	5.15	1.35	1.93	2.32	1.95	3.74

Seismic frames

Record	Bare frames		Fully infilled		Open story	
	δ_{top} (%)	COD	δ_{top} (%)	COD	δ_{top} (%)	COD
CAL0-35	0.97	1.29	0.12	1.33	0.23	3.00
CAL40S	1.19	1.26	0.06	1.00	0.43	2.44
CALITWE	1.10	1.39	0.12	1.33	0.37	2.83
CRU230	1.35	1.34	0.20	1.55	0.52	2.50
YPT330	2.34	1.32	0.18	1.56	0.68	2.51
RRS318	2.47	1.52	0.67	1.63	1.51	3.13

Table 6: Mean and standard deviation of COD.

Frame		mean ± SD	COV
Non-seismic	Bare	1.35 ± 0.09	0.07
	Fully infilled	1.74 ± 0.28	0.16
	Open story	3.50 ± 0.24	0.07
Seismic	Bare	1.35 ± 0.09	0.06
	Fully infilled	1.40 ± 0.21	0.15
	Open story	2.74 ± 0.27	0.10

Since the COD was found to be a fairly stable quantity for each of the considered configuration (its coefficient of variation ranges between 0.06 and 0.16), it is valuable for the prediction of the maximum interstory drift demand, given that a reliable estimation of Δ_{top} can be provided.
In the following, the comparison is presented between Δ_{top}, obtained from the dynamic analyses, and the displacement demand imposed to an elastic SDOF system.

Hysteretic Energy Demand

The hysteretic energy, which is a measure of inelastic energy dissipation demanded by the seismic excitation, includes cumulative effects of repeated cycles of inelastic response and can be associated to the expected structural and non structural damage (Bertero & Uang [8]). In this study the cumulative hysteretic energy per unit mass at the end of the excitations is considered.
The energy dissipated through inelastic deformation and/or cracking of the masonry infills, reported in Table 7, is strongly dependent on the ground acceleration time histories and on the mechanical and dynamic characteristics of the structures. In general, as expected, the dissipated energy increase with the ground motion damage potential, but its trend is also strongly affected by the structural system considered (seismic, non-seismic, bare, fully infilled and open story).

Table 7: Hysteretic dissipated energy at the end of the analyses, EH (cm^2/s^2).

Record	Non-seismic frames			Seismic frames		
	Bare	Fully infilled	Open story	Bare	Fully infilled	Open story
CAL0-35	710	2275	5409	2200	---	740
CAL40S	690	1380	3016	1075	---	860
CALITWE	1180	3720	8530	5060	---	1700
CRU230	2915	2485	2420	2593	1650	2180
YPT330	13275	4660	>2440	7880	1220	4809
RRS318	7590	12980	14778	14315	5885	18177

The influence of the structural characteristics varies considerably with the signal. In fact, the ratio between the hysteretic energy dissipated in the seismic frames and that dissipated in the non-seismic frames are in the following ranges: 0.60-3.10 for the bare frames, 0-0.70 for the fully infilled frames and 0.15-1.25 for the open story frames. While the ratio of dissipated energy in the fully infilled and open story frames on that dissipated in the bare frames are in the ranges 0-0.60 and 0.35-1.30 for the seismic frames and in the ranges 0.35-3.20 and 0.85-7.60 for the non-seismic frames. This values highlight the great variability and the lack of clear trends, thus displaying that results obtained through the amplification of a single natural accelerogram or with spectrum-compatible artificial signals, cannot be generalized.

In Figure 6 there are shown the percentages of energy dissipated by the beams, the columns and the infills in the open story frames; it is interesting to note that, in the non-seismic frame, energy is mainly dissipated in the first story columns, where plastic hinges occur at both ends, while in the seismic frame a greater amount is dissipated by the infills. In the seismic frame, the concentration of the drift at the first story is less marked than in the non-seismic and the presence of a drift demand in the higher stories leads to the cracking of masonry, with consequent dissipation of energy.

For the fully infilled frames, most of the dissipation occurs in the masonry panels, reducing the energy dissipation demand in the structural elements, and often preventing the development of plastic hinges.

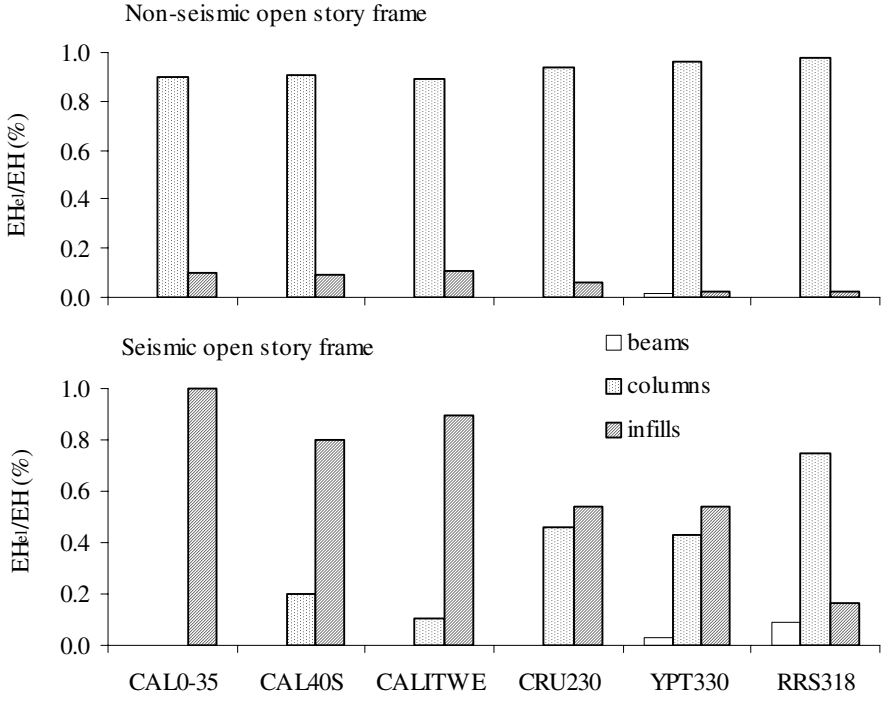

Figure 6: Energy dissipated in beams, columns or infills, EH_{el}, on total dissipated energy, EH.

Comparison Between MDOF and SDOF Demand

Usually, the evaluation of the demand for multi-degree-of-freedom (MDOF) systems is based on the demand for single-degree-of-freedom (SDOF) systems by means of response spectra.

In this paper, the comparison between MDOF and SDOF is performed for displacement demand and energy demand, considering 5% damped elastic displacement spectra, S_d, and 5% damped elastic input energy spectra, EI. The use of elastic displacement spectra is justified by the fact that in the range of periods of the analyzed structures, and for the soil type where the recording stations are located - intermediate soil with the only exception of YPT330, for which the use of an inelastic spectra could be more appropriate - the inelastic and elastic displacement are similar. Moreover, the adoption of different hysteretic behaviors slightly affect the above ratio (Decanini et al. [9]).

The comparison with SDOF systems requires the choice of appropriate periods. In Table 8 there are shown the fundamental vibration period determined by means of linear modal analyses, T_0, and the secant periods obtained through pushover nonlinear analyses, T_y and T_l, corresponding: the former to the yielding, the latter to the considered drift limits. The results presented in the following correspond to the adoption of the period T_l.

Table 8: Vibration periods of the test structures.

Frame		T_0 (s)	T_y (s)	T_l (s)
Non-seismic	Bare	1.38	1.52	1.60
	Fully infilled	0.16	0.51	0.91
	Open story	0.59	0.75	1.03
Seismic	Bare	0.73	0.86	1.09
	Fully infilled	0.14	0.49	0.74
	Open story	0.40	0.59	0.81

The following ratios are evaluated:

$$\frac{\Delta_{top}}{S_{d(\xi=0.05)}}$$

$$\frac{v_{EH-MDOF}}{v_{EI-SDOF}} = \frac{\sqrt{EH_{MDOF}}}{\sqrt{EI_{SDOF(\xi=0.05)}}}$$

where $v_{EH\text{-}MDOF}$ and $v_{EI\text{-}SDOF}$ are energy equivalent velocities ($E=(1/2)mv^2$), the former being the hysteretic energy equivalent velocity evaluated for the structures, the latter being the input energy equivalent velocity for the SDOF system. For SDOF systems, the ratio between hysteretic and input energy for the considered soil type condition is, on the average, in the range 0.42-0.72 depending on the reached ductility level (Decanini & Mollaioli [10]), thus its square root is in the range 0.69-0.85.

Figure 7 shows the above ratios for the six accelerograms, while Table 9 shows their mean, standard deviation, SD, and coefficient of variation, COV. The ratio $\Delta_{top}/S_{d(\xi=0.05)}$ presents a clear trend with the type of frame, the largest value being obtained for the bare frames, where the top displacement is, on the average, 1.83 for the non-seismic and 1.69 for the seismic frames. For the open story frames this ratios decrease to 1.19 and 0.86 for the non-seismic and for the seismic frame, respectively. A further decrease occurs for the fully infilled frames, where the top displacements are always smaller of those corresponding to the single-degree-of-freedom system, with the exception of the non-seismic frame subjected to the RRS318 record. It must be noted that great dispersions are found, especially for the bare and fully infilled non-seismic frames and for the fully infilled seismic frame. This situation would suggest that, when assessing the displacement demand in multi-degree-of-freedom systems, design displacement spectra with an high probability of non exceedance should be adopted.

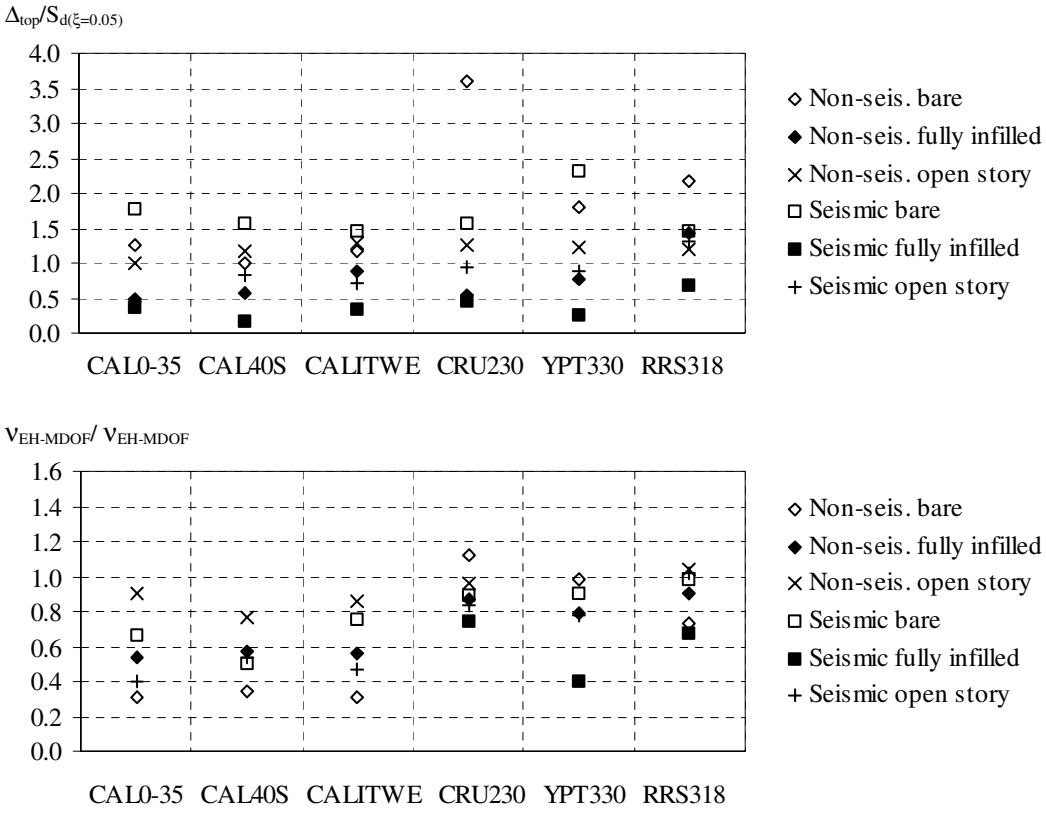

Figure 7: MDOF on SDOF ratios: $\Delta_{top}/S_{d(\xi=0.05)}$ and $\nu_{EH\text{-}MDOF}/\nu_{EI\text{-}SDOF}$.

Table 9: Mean, standard deviation and COV for $\Delta_{top}/S_{d(\xi=0.05)}$ and $\nu_{EH\text{-}MDOF}/\nu_{EI\text{-}SDOF}$ ratios.

Frame		$\Delta_{top}/S_{d(\xi=0.05)}$		$\nu_{EH\text{-}MDOF}/\nu_{EI\text{-}SDOF}$	
		mean ± SD	COV	mean ± SD	COV
Non-seismic	Bare	1.83 ± 0.97	0.53	0.63 ± 0.36	0.57
	Fully infilled	0.78 ± 0.34	0.44	0.70 ± 0.17	0.24
	Open story	1.19 ± 0.10	0.08	0.90 ± 0.10	0.18
Seismic	Bare	1.69 ± 0.33	0.20	0.78 ± 0.18	0.23
	Fully infilled	0.39 ± 0.18	0.47	0.61 ± 0.18	0.30
	Open story	0.86 ± 0.28	0.33	0.67 ± 0.24	0.36

Mean $\nu_{EH\text{-}MDOF}/\nu_{EI\text{-}SDOF}$ ratio ranges between 0.61 and 0.90, without a clear trend. Anyway, considering the mean plus one standard deviation, the equivalent velocity ratio is always smaller or equal to 1, i.e. the hysteretic energy demanded to the MDOF systems is smaller or equal to the elastic input energy for SDOF system with an equivalent period equal to T_I. The coefficient of variations present an high value for the bare non-seismic frame while for the other structural types it ranges between 0.18 and 0.36.

Damage Evaluation

With the aim of evaluating the structural damage level, a comparison between demands and capacities is carried out in terms of dissipated energy and interstory drift. Specifically, the damage level is herein evaluated by means of the following Combined Damage Index, CDI (Liberatore [11]):

$$CDI = a\left(\frac{Demand}{Capacity}\right)_{Drift} + b\left(\frac{Demand}{Capacity}\right)_{Energy} = a\frac{\delta_{max}}{\delta_{lim}} + b\frac{EH}{C_{EH}}$$

where the demand terms, δ_{max} and EH, derive from the nonlinear dynamic analyses, while "a" and "b" depend on the structural system. In the present study they are both set equal to 0.5.
The interstory drift limits, δ_{lim}, define a limit state associated to a high level of damage, i.e. a state in which the structure cannot withstand further significant ground motions and its capacity to sustain the vertical loads is reduced. The interstory drift limits are determined on the basis of: observed damage suffered by RC buildings during past severe earthquakes; rotational capacity of structural members, derived from analytical and experimental results; presence of infills; data obtained from several nonlinear dynamic analyses on RC models and values suggested by usual code prescriptions for the limitation of the interstory drift. The values adopted for the drift limits are shown in Table 10.
The hysteretic dissipation capacity, C_{EH}, evaluated through nonlinear pushover analysis, is:

$$C_{EH} = \int_{\Delta topy}^{\Delta topu} V_b(\Delta_{top})d\Delta_{top}$$

where V_b is the total base shear, Δ_{topy} is the top displacement corresponding to a conventional first yielding determined from an energetic equivalence with an elastic-perfectly-plastic single-degree-of-freedom system and Δ_{topu} is the ultimate top displacement. The values of Δ_{topu} are related to the attainment of the concrete ultimate strain for the bare and open story frames, and of the drift limit for the fully infilled frames.
In Table 10 there are reported δ_{lim}, Δ_{topy}, Δ_{topu} and C_{EH}, and in Table 11 the CDI.

Table 10: Drift limit, δ_{lim}, top displacements Δ_{topy}/H and Δ_{topu}/H, hysteretic dissipation capacity, C_{EH}.

Frame		δ_{lim} (%)	Δ_{topy} /H	Δ_{topu} /H	C_{EH} (cm^2/s^2)
Non-seismic	Bare	2.5	1.16	2.19	1365
	Fully infilled	1.5	0.37	1.24	3670
	Open story	1.8	0.22	0.46	510
Seismic	Bare	2.5	0.87	2.98	7330
	Fully infilled	1.5	0.44	1.24	4280
	Open story	1.8	0.23	0.77	2285

Table 11: Damage index CDI

Record	Non-seismic frames			Seismic frames		
	Bare	Fully infilled	Open story	Bare	Fully infilled	Open story
CAL0-35	0.72	0.51	> 2.00	0.40	0.05	0.34
CAL40S	0.66	0.38	> 2.00	0.37	0.02	0.46
CALITWE	0.95	0.81	> 2.00	0.65	0.05	0.62
CRU230	1.81	0.56	> 2.00	0.54	0.30	0.78
YPT330	> 2.00	0.95	> 2.00	1.16	0.24	1.39
RRS318	> 2.00	> 2.00	> 2.00	1.73	1.05	> 2.00

Based on the analysis of: (i) hinges distribution at the end of the accelerograms, (ii) maximum plastic hinges rotations and (iii) infill masonry strength degradation, values of CDI equal to 1 are related to a near collapse or partial collapse situation, while values of CDI greater than 2 correspond to complete collapse. Values ranging between 1 and 2 correspond to increasing probability of complete collapse. CDI greater than 2 are reported in Table 11 in bold letters. A great difference between non-seismic and seismic frames

is highlighted. In the seismic frame, the CDI is greater than 2 only for the RRS318 record, and there are very slight differences between bare and open story frame. In the non-seismic frames, the presence of the uniformly distributed infills is essential for the survival of such structures, while the presence of the open story, as already observed, is strongly harmful.

The attempt to correlate the damage level (CDI) to the strong motions parameters reported in Table 3 lead to the following considerations. The PGA gives bad estimations of the damage level, PGA is similar for the CRU230 and RRS318 records, while the corresponding damage levels are noticeably dissimilar, moreover YPT330 PGA is more than 20% smaller than CRU230 PGA, nevertheless the former produces a higher damage level. The PGV is better correlated to the structural damage. A better correlation for the seismic frames is obtained when considering the following product: $PGV\sqrt{AEI(0-2)}$, while for the non-seismic frames a good correlation is difficult to find, especially for the open story system as shown in Figure 8, where the CDI against the above product is shown.

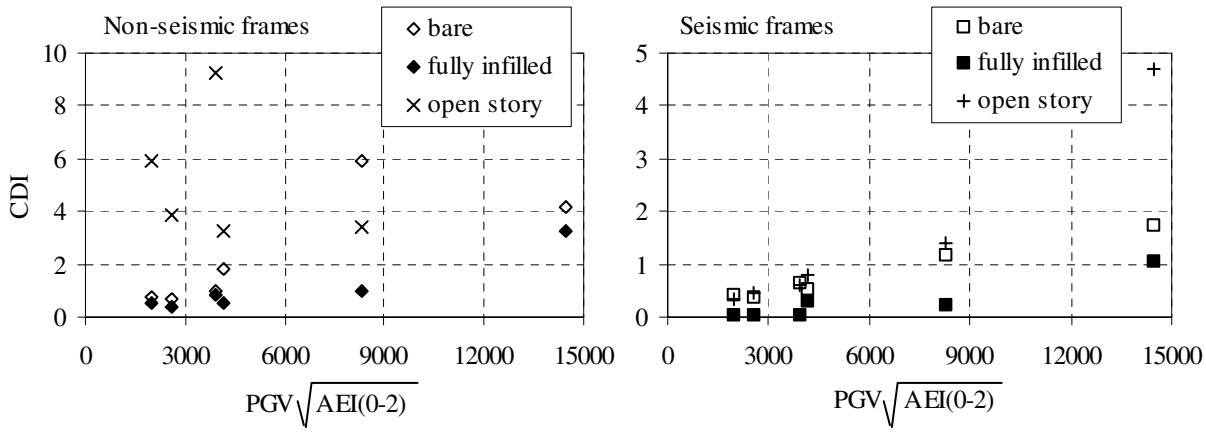

Figure 8: Comparison CDI - $PGV\sqrt{AEI(0-2)}$

CONCLUSIONS

The present study attempts to evaluate: (i) the behavior of reinforced concrete structures designed with no seismic actions, compared with aseismic structures and (ii) the effect of the influence of infill masonry panels and of their possible irregularities. The main conclusions is that the effect of infills on the seismic performance is beneficial, provided that infill panels retain most of their strength under cyclic loads. Field observations and tests results (Fardis ed. [12]) show that confinement provided by the surrounding frames is usually enough to keep in place infill panels of typical quality construction, allowing their good cyclic behavior. Under this conditions the structures benefit a lot from the energy-absorption capacity of infills and from the noticeable decrease of the lateral displacement demand. Anyway, it is worthwhile to mention that a masonry "stronger" than that considered in the present study could cause brittle failure mechanisms in the columns of the non-seismic structures. Moreover, the presence of an open story is strongly detrimental for the non-seismic frame, while the seismic structure is less affected by this irregularity in the infills distribution.

A first attempt is made to correlate the displacement and energy demand for MDOF systems with the demand for SDOF systems, one of the main difficulty being the choice of an appropriate period. The results obtained in the present study show that the top displacements are, on average, 1.76 (bare frames), 1.02 (open story frames) and 0.58 (fully infilled frames) times the displacement of the SDOF systems. However, great dispersion are found. The hysteretic energy demanded to the analyzed structures is found always smaller or equal to the spectral elastic input energy, but more accurate investigations are needed to

correlate the energy demand for MDOF systems and SDOF systems. Future development should involve, for example, the use of SDOF systems with different hysteretic behaviors.
With the aim of evaluating the structural damage levels a global damage index, which involve the evaluation of drift and hysteretic energy demands and capacities, is adopted. The comparison between the damage levels and the seismic input confirmed the difficulty in finding a unique parameter to describe the earthquake destructiveness, especially for the non-seismic frames. Overall, among the considered parameters, the PGV and the energetic parameters were found to provide the best correlation.

ACKNOWLEDGEMENTS

This study was performed within the research activity supported by the Ministry of Education, University and Research (MIUR).

REFERENCES

1. Pires F. M. “Influência das paredes de alvenaria no comportamento de estrututras reticuladas de betão armado sujeitas a acções horizontais”. PhD Dissertation. Laboratorio Nacional de Engenharia Civil, Lisbon 1990.
2. Kent D. C, Park R. “Flexural members with confined concrete”. Journal of Structural Division, ASCE. 1971, Vol. 97, No. ST7: 1969-1990.
3. Decanini L. D, Gavarini C, Bertoldi S. “Telai tamponati soggetti ad azioni sismiche un modello semplificato confronto sperimentale e numerico”. Atti del 6° Convegno Nazionale L’ingegneria sismica in Italia: 815-824. Perugia 1993.
4. Park Y. J, Reinhorn A. M, Kunnath S. K. “IDARC: Inelastic Damage Analysis of Reinforced Concrete Frames - Shear-Wall Structures”. Technical Report NCEER-87-0008, Sate University of New York at Buffalo 1987.
5. Decanini L. D, Mollaioli F. “Formulation of Elastic Earthquake Input Energy Spectra”. Earthquake Engineering and Structural Dynamics 1998; vol.27: 1503-1522.
6. Negro P, Verzelletti G. “Effect of infills on the global behaviour of R/C frames: energy consideration from pseudodynamic tests”. Earthquake Engineering and Structural Dynamics 1996; Vol. 25, 753-773.
7. Panagiotakos T. B, Fardis M. N. “Effect of column capacity design on earthquake response of reinforced concrete buildings”. Journal of Earthquake Engineering. Vol. 2 No. 1 (1998) 113-145.
8. Bertero V. V, Uang C. M. “Issues and future directions in the use of energy approach for seismic-resistant design of structures”. Nonlinear Seismic Analysis and Design of Reinforced Concrete Buildings. Fajfar P. and Krawinkler H. editors. Elsevier Applied Science 1992; 3-22.
9. Decanini L. D, Liberatore L, Mollaioli F. “Characterization of displacement demand for elastic and inelastic SDOF system” Soil Dynamics and Earthquake Engineering 23 (2003) 455-471.
10. Decanini L. D, Mollaioli F. “An energy-based methodology for the assessment of seismic demand” Soil Dynamics and Earthquake Engineering 21 (2001) 113-137.
11. Liberatore L. “Aprocci innovativi in termini di energia e di spostamento per la valutazione della risposta sismica di strutture a più gradi di libertà”. PhD Dissertation, Università di Roma “La Sapienza”, Italy 2001.
12. Fardis M. N. (ed.) “Experimental and Numerical Investigations on the Seismic Response of RC Infilled Frames and Recommendations for Code Provisions”. ECOEST/PREC8 report No.6, Laboratorio Nacional de Engenharia Civil, Lisbon 1996.